Stellar Spectra and Atmospheric Composition

P. B. HAYS AND R. G. ROBLE

Dept. of Aerospace Engineering, University of Michigan, Ann Arbor

(Manuscript received 16 January 1968, in revised form 22 July 1968)

ABSTRACT

The distortions to the image and spectrum of a star being observed during occultation from a satellite are discussed. The primary distortions are shown to be due to refractive dispersion, small and large particle scattering, and absorption by various atmospheric gases. Representative stellar spectra in both the visible and ultraviolet are presented, and various features relating to specific atmospheric constituents are discussed. The possibility of recovering information concerning atmospheric composition from stellar spectra is considered and several distinct processes are used for illustration.

1. Introduction

The earth's atmosphere is the cause of considerable inconvenience to the astronomer since it acts as a complex prism, refracting, absorbing and dispersing light from extraterrestrial objects in a manner analogous to a conventional spectroscope. However, these effects which are so troublesome to astronomers can be of considerable use to the geophysicist in determining the structure and composition of the atmospheres of the earth and planets, especially if optical observations of an extraterrestrial light source are made during occultation from a nearby satellite.

The first analysis of the occultation technique for obtaining atmospheric structure was performed by Pannekoek (1903) who considered the occultation of a star by a planet as observed from a ground based observatory. Baum and Code (1953) applied the technique to the occultation of Sigma Arietis by Jupiter and were thus able to determine a scale height for the upper atmosphere of Jupiter. Weisberg (1962) also considered this technique as a method of sounding an atmosphere by measuring the extinction of occulting stars observed from a satellite. All of these authors considered refractive dispersion as the dominant attenuation process and used broadband photometric data to obtain atmospheric information. Other investigators (Venkateswaran *et al.*, 1961; Johnson *et al.*, 1951; Hinteregger *et al.*, 1965) have used the sun as an extraterrestrial source and have obtained atmospheric data from information obtained during occultation. A difficulty with the sun as an extraterrestrial source is that rays from its 0.5° disk extend over 20 km at the tangent point for normal satellite altitudes making fine atmospheric structure difficult to retrieve. Even if only a small portion of the sun's disk is used to sharpen the resolution at the tangent point, only sunrise and sunset are still available for making measurements—times during which the atmosphere is undergoing rapid change. This is particularly important when mesospheric ozone is being considered due to the rapid changes in ozone density which occur in twilight. Jones *et al.* (1962) and Fischbach (1965) have discussed a technique for measuring the structure of the earth's stratosphere which utilizes a continuous recording of the angular refraction of starlight from a satellite. Since stars are point sources the resolution at the tangent point is greatly increased and since occultation of a star from a tangent ray height of 100 km occurs in 30 sec, many observations may be made during an orbit and global coverage may be obtained.

In this paper we will analyze the image shape and spectral distribution of starlight passing tangentially through an atmosphere and show how the resulting spectral and image distortions may be utilized to obtain geophysical information on the structure and composition of an atmosphere. We will examine, in particular, stellar occultations observed from a satellite for which it is possible to obtain a unique mathematical inversion, recovering atmospheric properties at the tangent point from the occultation data (Hays and Roble, 1968). The analysis presented assumes spherical symmetry throughout. This assumption is valid for all features having a horizontal scale of a few hundred kilometers.

2. Refraction

The refraction angle of a star, when viewed from outside a spherically stratified atmosphere, obeys the equation

$$R(\mu_0 r_0) = 2\mu_0 r_0 \int_{\mu_0 r_0}^{\infty} \frac{\dfrac{d \log \mu}{d(\mu r)} d(\mu r)}{\sqrt{(\mu r)^2 - (\mu_0 r_0)^2}}, \qquad (1)$$

where μ is the index of refraction, r the radial distance

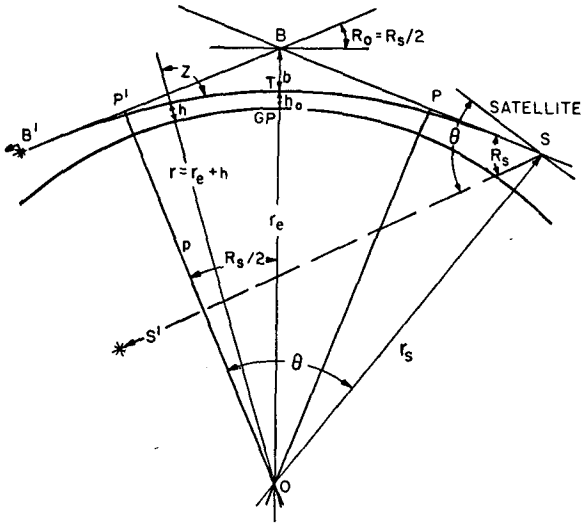

FIG. 1. Geometry of refraction. The angle θ should be θ_s.

from the center of the planet to the ray path, and the subscript 0 refers to the point of closest approach to the planet, the tangent point. The geometry of refraction is illustrated in Fig. 1. The method of extracting information about the atmosphere from optical observations of the refracted star image is based upon the fact that a knowledge of the refraction angle as a function of the position of the star above the horizon is entirely sufficient to determine the index of refraction as a function of height above the planetary surface. Since one knows the composition of the earth's lower atmosphere, the density is obtained directly from the scan of the stellar refraction angle.

Mathematically, this process is entirely analogous to the investigation of the propagation of seismic waves and the determination of the structure of the solid earth as discussed by Bateman (1910), which has received considerable attention from the geologist. Rays of starlight, as well as seismic rays, are brachistochrones and both traverse spherically stratified media; consequently, they obey Snell's law,

$$\mu_0 r_0 = \mu r \sin Z = \text{constant}. \tag{2}$$

Thus, since the measurement is carried out from a satellite at $r=r_s$, $\mu_s=1.0$, and knowing Z_s at the satellite, the refraction angle is known in terms of the parameter

$$\mu_0 r_0 = r_s \sin Z_s. \tag{3}$$

The refraction equation (1) is an Abel integral equation and allows the simple inversion

$$\mu = \exp\left\{-\frac{1}{\pi}\int_{ur}^{\infty} \frac{R(\mu_0 r_0)\,d(\mu_0 r_0)}{\sqrt{\mu_0^2 r_0^2 - \mu^2 r^2}}\right\}, \tag{4}$$

yielding the index of refraction as a function of the distance above the surface of the planet. The use of Gladstone and Dale's law allows one to obtain the atmospheric density directly from the index of refraction

$$\mu = 1 + k(\lambda)\rho, \tag{5}$$

where $k(\lambda)$ is a dispersion parameter for air and ρ is the mass density of the atmosphere. The above relations apply to monochromatic light; the result of examining a rather broad spectral band complicates the process but does not fundamentally affect the result.

It is useful to record a simple approximation to the refraction angle (1) for an exponential atmosphere, i.e.,

$$R(r_0,\lambda) = k(\lambda)\rho(r_0)\sqrt{\frac{2\pi r_0}{H}}, \tag{6}$$

where H is the scale height. The prediction of refraction angles from (6) is good to a few per cent and consequently will yield results of sufficient accuracy for our purposes when considering the dispersion and attenuation which result from refraction. For comparison, the refraction angle as a function of tangent ray height for light of wavelength $\lambda=7000$ Å is tabulated in Table 1 for various model atmospheres. The exponential approximations are obviously suitable for most computations.

TABLE 1. Refraction angle in arc seconds for various atmospheric models.

Tangent ray height (km)	CIRA 1965	Local exponential approximation	Isothermal based on CIRA at 10 km
5	2412.28	2514.38	3337.89
10	1534.62	1519.77	1529.87
15	756.37	732.03	701.24
20	335.18	326.31	321.36
25	148.55	144.92	147.31
30	67.428	65.798	67.531
35	31.063	30.115	30.939
40	14.442	13.947	14.185

3. Dispersion and attenuation of visible light

The dispersion and attenuation of the short wavelength radiation coming from an occulting star can be conveniently discussed by separating the spectral region into the visible and ultraviolet. Here we include the near ultraviolet and near infrared in the visible spectrum and all shorter wavelengths in the ultraviolet. The visible spectral region is distorted primarily by the dense portions of the earth's atmosphere, the troposphere and stratosphere, where scattering, refractive attenuation and distortion, and ozone absorption in the Chappuis band are predominant features. In this region of the atmosphere, the ultraviolet is almost entirely absorbed. The ultraviolet region of the spectrum is of interest for rays of light which penetrate the more tenuous fringes of the atmosphere, the mesophere and thermosphere of the earth, where the visible spectra is transmitted

without distortion. These shorter wavelengths have sufficient energy to cause dissociation and ionization of various constituent gases; as a consequence, the dissociation and ionization spectra of a number of atmospheric constituents appear in the transmitted stellar spectra. The following discussion will be divided according to these two physically distinct spectral and atmospheric regions. Although the atmosphere of the earth will be used as the primary example, the results obtained here are nearly all directly applicable to other planetary atmospheres as well.

When light passes through a large air mass, as it must when an occulting star is viewed near the horizon, the most significant processes affecting the transmitted light are those which have small attenuation cross sections, or which are caused by very minor constituents. Any major attenuation process causes the atmosphere to be opaque in the affected spectral region. In the earth's atmosphere, Rayleigh or molecular scattering, Mie scattering, as well as refractive dispersion and ozone absorption, provide the primary loss processes for visible light passing through the lower dense regions. Unfortunately, in the denser regions of the atmosphere one cannot consider these effects separately. Refraction causes the individual rays of light to follow curved paths and is thus intimately connected with the total number of particles along a given ray. This is particularly significant since the index of refraction is dependent on the wavelength, which causes rays from different spectral regions to follow separate paths through the atmosphere.

In general, a ray of light of wavelength λ suffers attenuation

$$\frac{I(\lambda,r_0)}{I_\infty(\lambda)}=\exp\left\{-\sum_i \oint_{-\infty}^{\infty}\sigma_i N_i(s)ds\right\}\Psi(\lambda,r_0), \quad (7)$$

where $I_\infty(\lambda)$ is the intensity in the absence of attenuation, $I(\lambda,r_0)$ is the intensity of the ray after passing through the atmosphere with tangent height or radial distance r_0 (from Fig. 1, $r_0=r_e+h_0$), σ_i the cross section for scattering or absorption, N_i the number density of ith species, and $\Psi(\lambda,r_0)$ the change in intensity due to refractive dispersion of the light. Here the integration is carried out along the path of the refracted light and ds is the element of length along this path (see Fig. 1). The major result of refraction on the path of a given ray of light is to change the height of the point of tangency of the ray. Since the curvature is small, it is usually sufficient to treat the ray as though it were a straight line passing tangent to the planet at a height r_0 which is determined by refraction.

The tangent height of a given ray of wavelength λ when viewed from outside the atmosphere is determined by the angular position and height of the observer and by the wavelength of the ray of light. All rays observed at the position r_s, θ_s of the satellite observer must intersect at that point; that is, from the geometry illustrated in Fig. 1, the angle θ_s is a constant for all rays, where

$$\theta_s=\pi+R(\lambda,r_0)-\sin^{-1}\left\{\left(\frac{r_0+b}{r_s}\right)\cos^{-1}\left(\frac{R(\lambda,r_0)}{2}\right)\right\}. \quad (8)$$

By using Snell's law (3), the Gladstone and Dale law (5), and expressing b in terms of μ_0, r_0 and R, one finds

$$\theta_s=\pi+R(\lambda,r_0)-\sin^{-1}\left\{\frac{r_0[1+k(\lambda)\rho_0]}{r_s}\right\}. \quad (9)$$

Here ρ_0 and $k(\lambda)$ refer to the major constituents which determine the angular refraction. In theory, this equation for r_0 could be solved in terms of λ, θ_s and r_s, but this is impractical and the process can be simplified by expanding the equation about a specific point r_0^* which is the tangent ray height for a ray with wavelength λ^*. This is possible whenever $k(\lambda)$ is a slowly varying function of wavelength. This leads to the result that

$$r_0(\lambda)=r_0^*+\Delta r_0(\lambda), \quad (10)$$

where

$$\Delta r_0(\lambda)=\frac{\left(\frac{\partial\theta_s}{\partial k}\right)_{r_0}}{\left(\frac{\partial\theta_s}{\partial r_0}\right)_k}[k(\lambda)-k(\lambda^*)]. \quad (11)$$

For an isothermal atmosphere

$$r_0(\lambda)=r_0^*+\left\{\frac{\rho_0^*\sqrt{\frac{2\pi r_0^*}{H}}\frac{r_0^*\rho_0^*}{\sqrt{r_s^2-\mu_0^{*2}r_0^{*2}}}}{\frac{2\pi(\mu_0^*-1)}{H}\left(\frac{-H+2r_0^*}{\sqrt{8\pi H r_0^*}}\right)+\frac{[\mu_0^*-(r_0^*/H)(\mu_0^*-1)]}{\sqrt{r_s^2-r_0^{*2}\mu_0^{*2}}}}\right\}[k(\lambda)-k(\lambda^*)]. \quad (12)$$

Thus, one observes for short wavelengths, where the index of refraction is larger, that the tangent ray height is higher than for longer wavelengths. This effect is illustrated in Fig. 2 where $\Delta h=\Delta r_0$ is presented as a function of the tangent ray height r_0^* and λ, for $\lambda^*=7000$Å for an observer 500 km above the earth.

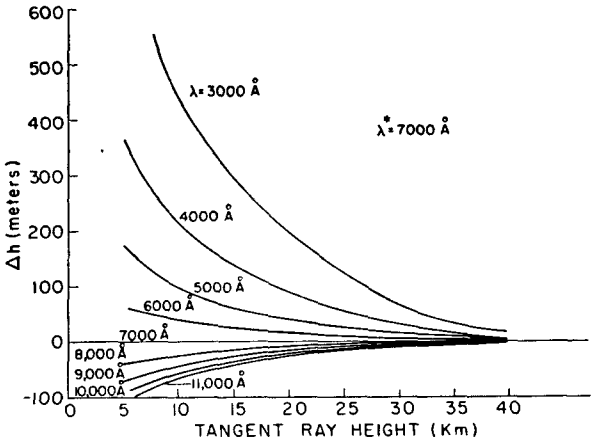

FIG. 2. Height difference Δh at the tangent point between base ray λ^* and ray corresponding to wavelength λ for various tangent ray heights for an observer 500 km above the earth.

Using these results, we can now discuss the effects of scattering and absorption on the intensity of transmitted star light.

a. Refractive dispersion

The distortion of the planar wave front, due to refraction, as the light passes through the atmosphere causes changes in intensity of the transmitted radiations. This change in intensity is due to the variation in cross-sectional area of a bundle of light rays as it passes through the atmosphere. From the geometry in Fig. 1, we find the intensity reduction to be

$$\Psi(\lambda,r_0)=\left(\frac{p}{|r_s\sin\theta_s|}\right)\times\left\{\frac{\cos R}{\left|1+\frac{\partial}{\partial r_0}\left[\tan R\left(r_s\cos\theta_s-p\sin\frac{R}{2}\right)\right]\right|}\right\}; \quad (13)$$

on neglecting terms of the order R^2 and considering an observer near the earth or a planet, (13) becomes approximately

$$\Psi(\lambda,r_0)=\frac{1}{1+r_s\cos\theta_s\left(\frac{\partial R}{\partial r_0}\right)}. \quad (14)$$

Since $r_s\cos\theta_s$ and $\partial R/\partial r_0$ are in general negative, the net result of differential refraction in the immediate vicinity of a planet is a reduction in intensity. The transmission function for refractive dispersion in the earth's atmosphere is illustrated in Fig. 3 for an observer 500 km above the earth's surface. Notice that the variation with wavelength is very slight and for practical purposes may generally be neglected. The isothermal approximation for the refractive dispersion is

$$\Psi(\lambda,r_0)\cong\frac{1}{\left[1-\frac{r_s\cos\theta_s}{H}\sqrt{\frac{2\pi r_0}{H}}k(\lambda)\rho_0\right]}. \quad (15)$$

This function is normally sufficiently accurate to predict the attenuation caused by refraction and certainly can be used to make any wavelength correction.

b. Molecular scattering

The transmission function due to scattering and attenuation for the case of starlight passing tangentially to a planet's atmosphere is

$$T=\frac{I(\lambda)}{I_\infty(\lambda)}=\exp\left\{-\int_{r_0(\lambda)}^{\infty}\frac{\sigma N(r)r\,dr}{\sqrt{r^2-r_0^2(\lambda)}}\right\}, \quad (16)$$

where $I(\lambda)$ is the transmitted intensity, $I_\infty(\lambda)$ the intensity of the star above the earth's atmosphere, σ the cross section of the scattering or absorption process, $N(r)$ the number of scatterers or absorbers at r, and $r_0(\lambda)$ the corresponding tangent ray height for wavelength λ.

The cross section for Rayleigh or molecular scattering for air (Allen, 1963) is

$$\sigma_R=\frac{32\pi^3k^2(\lambda)M}{3\lambda^4}, \quad (17)$$

where M is the mass of a hypothetical air molecule. The transmission function for an exponential, spherically stratified atmosphere resulting from Rayleigh scattering is

$$T_R=\exp\left\{-\left(\frac{32\pi^3}{3\lambda^4}\right)k^2(\lambda)M^2N_0(\lambda)\sqrt{2Hr_0(\lambda)}\right\}, \quad (18)$$

where r_0, N_0 are evaluated at the height $r_0(\lambda)$. We see

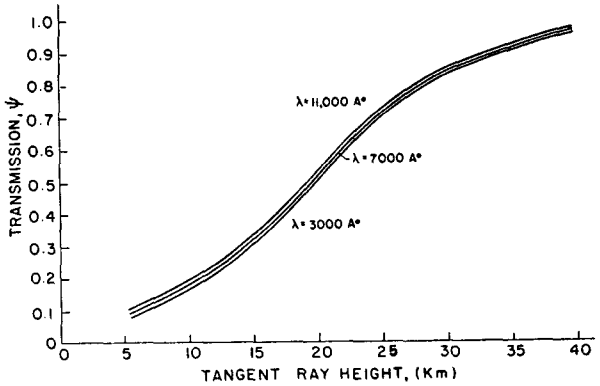

FIG. 3. Transmission function for refractive dispersion at various wavelengths in the earth's atmosphere for an observer 500 km above the earth. $\lambda^*=7000$ Å.

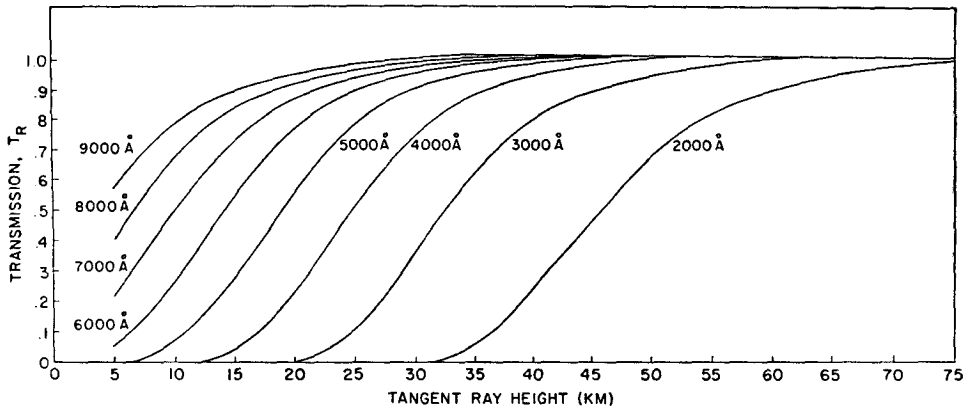

FIG. 4. Transmission function for molecular (Rayleigh) scattering at various wavelengths in an exponential atmosphere as a function of tangent ray height.

from this expression that the error due to neglecting the change in height of various wavelengths is rather small, i.e., of the order $\Delta r_0/H$ and generally less than 10% for the visible and near ultraviolet. This is due to the fact that the main atmospheric constituents change relatively slowly with height. The attenuation due to Rayleigh scattering is one of the factors that can be predicted quite accurately and, consequently, does not enter into consideration as an unknown to be determined; it is a factor, however, that must be removed from any experimental results before an analysis of the transmitted spectra can be made. The transmission function for Rayleigh scattering is shown in Fig. 4 as a function of tangent ray height and wavelength in an exponential atmosphere.

c. *Mie scattering*

The distribution of small particle scatterers such as large aerosols and Aitkin particles in the troposphere and stratosphere is not well known. Even the assumption of spherical stratification should be viewed with suspicion. However, Junge (1963) and Chagnon and Junge (1961) have presented the results of several experimental determinations of particle size distribution and profiles of the distribution of particles with height. Utilizing the empirical power law size distribution derived by Junge (1963) and incorporating the scattering coefficient approximation given by van de Hulst (1962), a mean cross section for Mie scattering is

$$\sigma_M(\lambda)=\pi\left(\frac{c}{2.3}\right)\left(\frac{\lambda}{2\pi}\right)^{2-\beta}$$
$$\times\int_{X_1}^{X_2}\left[2+\frac{4}{\xi}\sin\xi+\frac{4}{\xi^2}(1-\cos\xi)\right]X^{(1-\beta)}dx, \quad (19)$$

where $\xi=2x|(M'-1)|$, M' being the index of refraction of the particles, $x=2\pi r/\lambda$, where r is the particle radius, and c and β are constants used by Junge to characterize particle size distribution. Here X_1 and X_2 are the limits on the distribution of particle radii. To illustrate the region of major influence of aerosol scattering, the results of calculations of the Mie particle transmission function for the experimental distributions given by Junge (1963) are shown in Fig. 5. These results illustrate the variation of intensity with wavelength and tangent ray height due to Mie scattering alone. As expected, the loss due to these larger particles is not strongly dependent on wavelength.

d. *Ozone absorption*

In the visible region of the spectrum, the Chappuis band of ozone is the primary cause of direct photo-absorption. The photo-absorption cross section as a function of wavelength is well known and peaks near

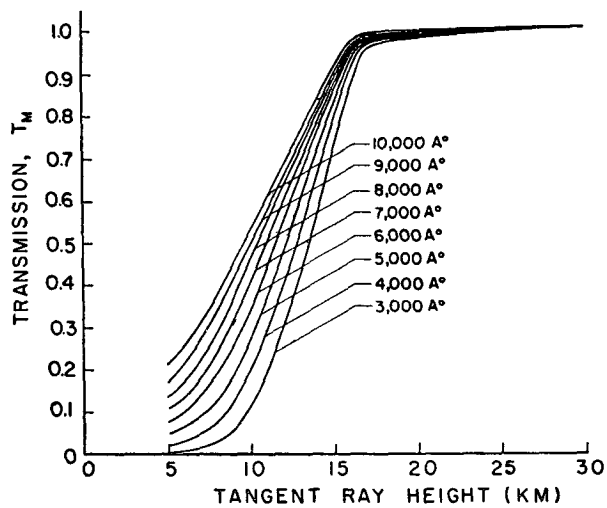

FIG. 5. Mie transmission function for particle scattering at various wavelengths as a function of tangent ray height for particle distributions by Junge (1953).

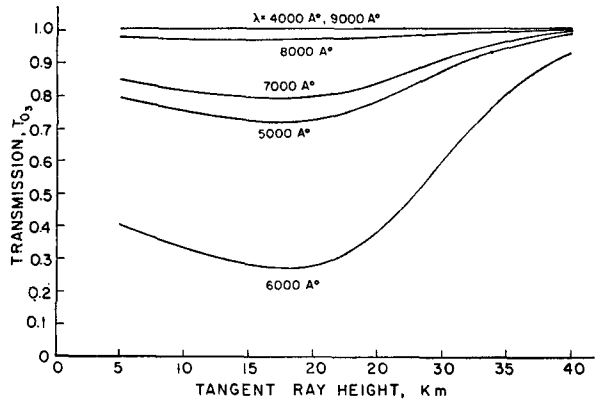

FIG. 6. Transmission function for ozone absorption in the Chappuis band using the ozone profile of Green (1964).

6000 Å. Although the distribution of ozone with height has been the subject of considerable study, it is not well known at present. These are as yet unexplained seasonal and latitudinal variations according to Hunt (1966) and Roney (1965) which seem to depend upon stratospheric circulation, but which may be related to water vapor distributions. For the purpose of illustration, we have taken as a typical ozone profile that given by Green (1964) in the form

$$N_{O_3}(r)=\frac{W_p}{h}\frac{\exp[(r-r_p)/h]}{\{1+\exp[(r-r_p)/h]\}}, \qquad (20)$$

where W_p, h and r_p are constants adjusted to give a reasonable standard ozone profile. Since lateral variations of ozone are gradual, spherical stratification can be assumed and the transmission function for ozone absorption is shown in Fig. 6 for the model ozone profile described. The strong attenuation in the center of the Chappuis band and the tendency for the attenuation to remain constant below the ozone peak is clearly illustrated. However, these results represent at best only a mean condition.

e. Minor contributions

There are several other minor contributions to attenuation in the lower atmosphere. Water vapor occurs primarily below the tropopause where clouds will generally interfere with transmitted light and will cause the apparent horizon to be above the region where water vapor itself is important. Atmospheric turbulence can contribute to the reduction in intensity and give rise to intensity fluctuations, but this effect is probably confined to the troposphere and should not cause serious attenuation above the cloud-top level. The result of any turbulence would be a refractive type of dispersion due to small scale irregularities in the index of refraction. Molecular oxygen has several minor absorption bands in the visible; however, these are narrow and should be of lesser importance than the factors previously discussed. The minor constituents CO_2, N_2O and CH_4 are of very little consequence in the visible region of the spectrum and may be ignored. Intense resonant line scattering such as the sodium doublet occupy such narrow spectral regions that they can also be neglected.

4. Visible spectra

The results obtained thus far allow us to discuss the visible spectrum of occulting stars for a mean atmosphere. We will adopt the empirical expression given by Allen (1963) to simulate the visible stellar spectrum above the atmosphere, i.e.,

$$I_\infty(\lambda)=\exp[-(0.921M_v+19.388)]\left(\frac{\lambda_0^5}{\lambda^5}\right)\times\frac{\left[\exp\left(\frac{1.438\times10^7}{\lambda_0 T}\right)-1\right]}{\left[\exp\left(\frac{1.438\times10^7}{\lambda T}\right)-1\right]}\times10^{-7}, \qquad (21)$$

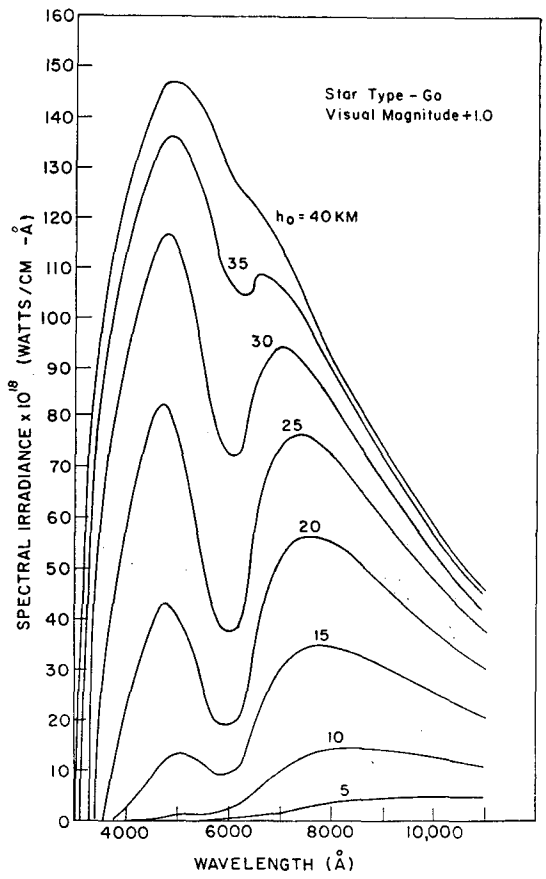

FIG. 7. Stellar transmission spectra as a function of tangent ray height at a reference wavelength $\lambda^*=7000$Å for a star with a blackbody temperature of 6000K.

where $\lambda_0 = 5500$Å, M_v is the visual magnitude, T the effective blackbody temperature of the star, and the units of $I_\infty(\lambda)$ are W cm^{-2} Å^{-1}. For the purpose of illustration, we have chosen a type G0 star of visual magnitude +1 with an effective blackbody temperature of 6000K. When the attenuating factors considered in the previous sections are combined with the assumed spectral distribution of the star, and due consideration is given to the fact that each wavelength corresponds to its individual tangent ray height around the base ray, then the transmission spectrum of the star may be calculated. The spectral distribution as a function of wavelength and tangent ray height (with reference wavelength at $\lambda^* = 7000$Å) is given in Fig. 7. Above 40 km there is little attenuation, but below that altitude the Chappuis band of ozone gives a prominent feature near 6000Å. As the altitude decreases, Rayleigh scattering intensifies in the shorter wavelength region causing the relative maximum around 5000 Å to decrease more rapidly than that at longer wavelengths. There is a general decay of the entire spectrum associated with refractive dispersion, Rayleigh scattering, and at lower altitudes, Mie scattering.

a. Shape of stellar images

We have also considered the shape of an image seen from an orbiting observatory. This question is of interest particularly in view of the suggestion that refraction angles be used directly to recover atmospheric structure. In Fig. 8 we have combined the spectral attenuation profile and the angular distribution of light between 3000 and 11,000Å, observed from a satellite at a height of 500 km, to give image contours. It can be seen that the initial point source of the star above the atmosphere is spread out into a line spectrum along the density gradient in the earth's atmosphere. Again the base ray is $\lambda_0^* = 7000$Å, and it is shown (Fig. 8) that along with the general energy decay due to the attenuating factors there is a broadening of the image as one proceeds lower in the atmosphere. The broadening is most pronounced in the blue end of the spectrum. The most prominent feature is the strong ozone absorption valley near 6000Å.

To determine the stellar shape which would be distributed over a typical photocathode surface, we have included in a second spectrum the spectral characteristics of a S-20 photocathode (Fig. 9), which has a good response over most of the region considered. The resulting images illustrate the general decay with tangent ray height due to the attenuating factors and show a general shift in the image centroid during occultation. This shift is quite significant and surely would have to be removed if star tracking of a few arc seconds were required.

5. Absorption of ultraviolet light during occultation

Although the less dense regions of the atmosphere have little influence on visible light, they do strongly

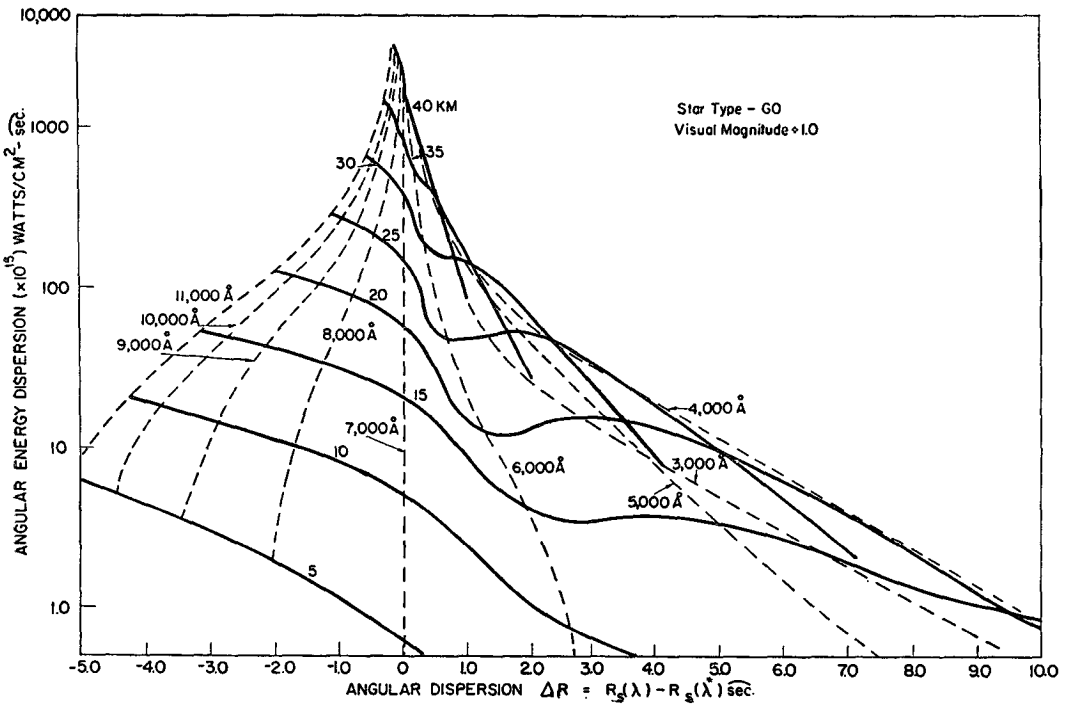

FIG. 8. Angular energy dispersion for various tangent ray heights during occultation using the stellar transmission function of Fig. 7 and the angular dispersion of light from 3000–11,000Å at a height of 500 km. $\lambda^* = 7000$Å.

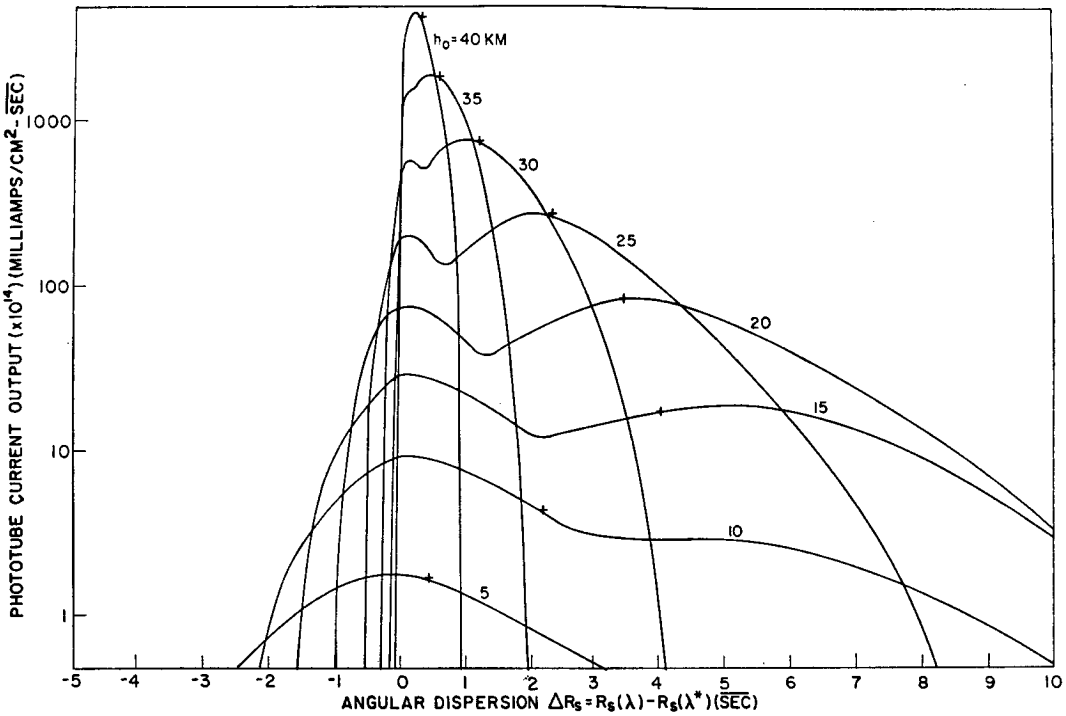

FIG. 9. S-20 photocathode star image for various tangent ray heights during occultation.

influence the ultraviolet portion of the spectrum. Of the factors previously discussed, only Rayleigh scattering and ozone absorption are influential at higher altitudes and shorter wavelengths, Rayleigh scattering due to the increase of the cross section at shorter wavelengths, and ozone due to the existence of the strong Hartley-continuum and Huggins absorption bands in the ultraviolet. In addition to these features, the dissociation and ionization spectra of molecular oxygen, atomic oxygen and other atmospheric gases become important. Here only the spectral region between 1200 and 3500Å, a region in which the influence of molecular oxygen and ozone predominates, will be discussed. The photo-absorption cross sections for these molecules are obtained from Watanabe (1958) and Ditchburn and Young (1962). The data in the Schumann-Runge band system of molecular oxygen for 1750–2000Å are poorly defined and consequently will not be used in the following discussion.

a. Rayleigh scattering

Fortunately, Rayleigh scattering in the earth's atmosphere is important only up to about 80 km, and thus can be predicted without great uncertainty. The transmission function for Rayleigh scattering is presented in Fig. 4, as discussed in Section 3b. Above 80 km its influence is negligible as an attenuating factor in the spectral region discussed here.

b. Ozone

Ozone is the dominant factor in determining the ultraviolet spectra between 2000 and 3500Å for rays of starlight passing through the mesosphere. However, the uncertainty in the mesospheric ozone profile is large. Large diurnal and seasonal variations occur in this region, but no adequate theoretical treatment of the ozone photochemistry is as yet available. The influence of small amounts of water vapor and associated hydrogen compounds appears to be very important, and above 80 km the complex ozone-atomic oxygen transport and photochemical processes cannot be adequately treated due to the lack of fundamental information concerning transport processes as well as a lack of accurate data on the rate coefficients for various important photochemical reactions.

To illustrate the variability of the influence of ozone on stellar spectra, four examples are presented in Figs. 10–13 showing the extreme diurnal variation of the ozone transmission function for theoretically predicted ozone profiles, with one pair for a pure oxygen atmosphere

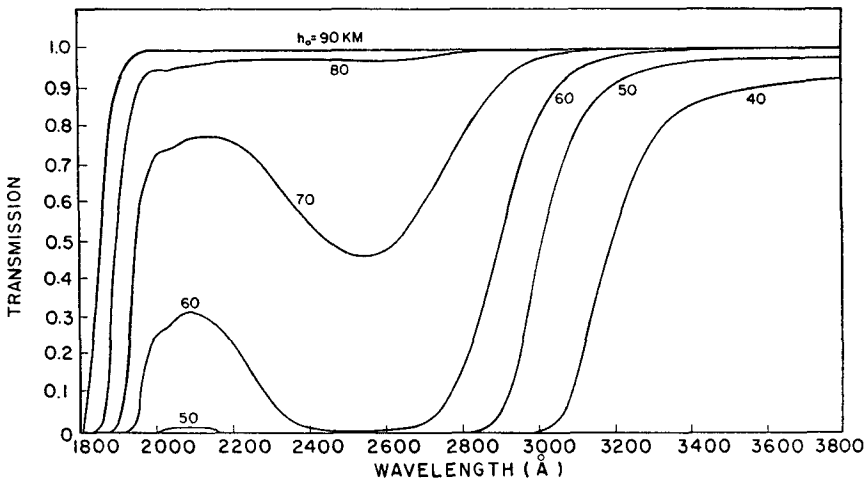

FIG. 10. Transmission function for the combined effects of molecular scattering, molecular oxygen absorption, and ozone absorption corresponding to Hunt's daytime ozone model.

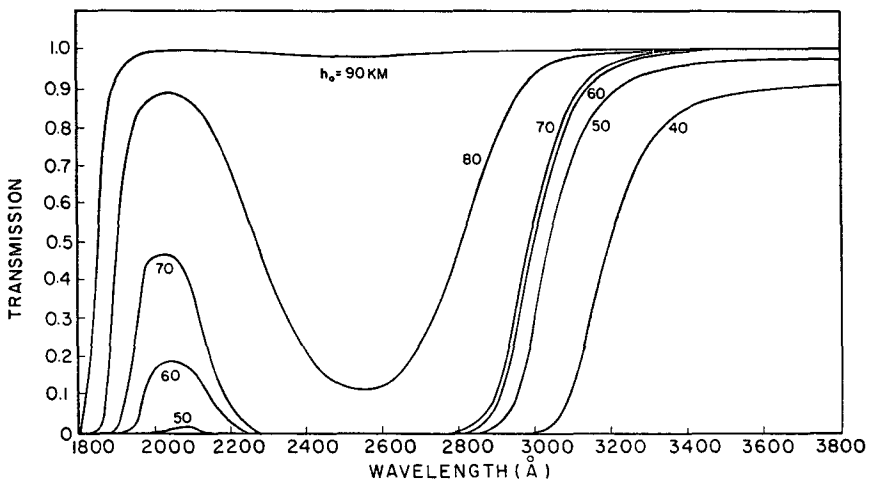

FIG. 11. Same as Fig. 10 except for Hunt's nighttime ozone model.

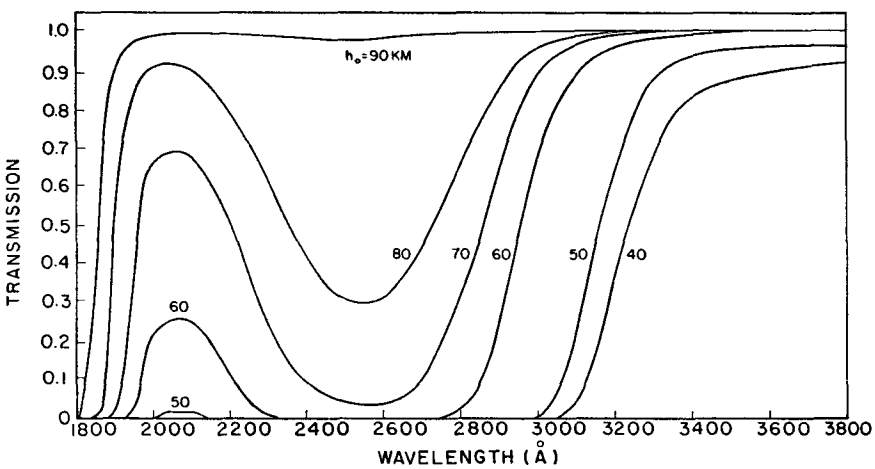

FIG. 12. Same as Fig. 10 except for London's daytime ozone model.

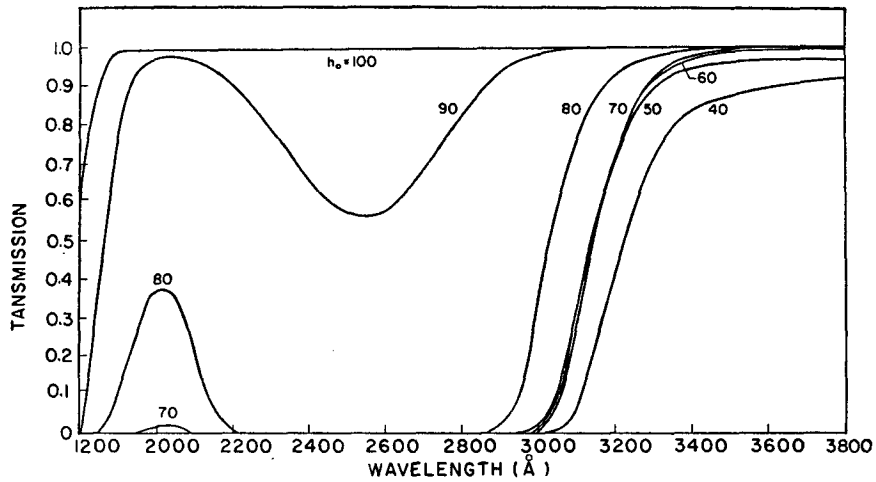

FIG. 13. Same as Fig. 10 except for London's nighttime ozone model.

(London, 1967) and a second pair for a moist atmosphere (Hunt, 1966). The effects of Rayleigh scattering and the Herzberg system of molecular oxygen is included in these spectra, but the contributions are minor and predictable in the mesosphere.

c. Molecular oxygen

Molecular oxygen, like ozone, is the subject of some uncertainty but in contrast to ozone the uncertainty is primarily in the thermosphere. In this case, the variability is associated with the complex dissociation, diffusion and recombination processes which occur near the "turbopause" region (Colegrove *et al.*, 1966). Actually, molecular oxygen, ozone and atomic oxygen are each individual aspects of a single phenomenon. However, molecular oxygen does not exhibit the large diurnal variation of ozone and, in this sense, its behavior is less complex.

In the upper thermosphere above 150 km, diffusive equilibrium prevails allowing the neutral gas temperature to be related to the molecular oxygen profile. The transmission function for molecular oxygen absorption between 1200 and 1700Å for the average atmosphere of Colegrove *et al.* is shown in Fig 14.

6. Ultraviolet spectra

Stellar class O and B stars with a high effective temperature have a blackbody emission spectrum peaking

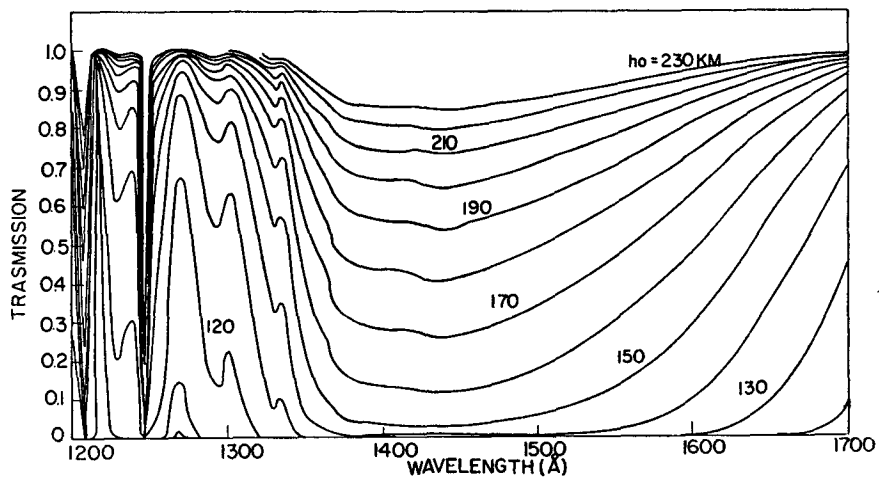

FIG. 14. Transmission function for molecular oxygen absorption corresponding to Colegrave *et al.* (1966) average molecular oxygen profile.

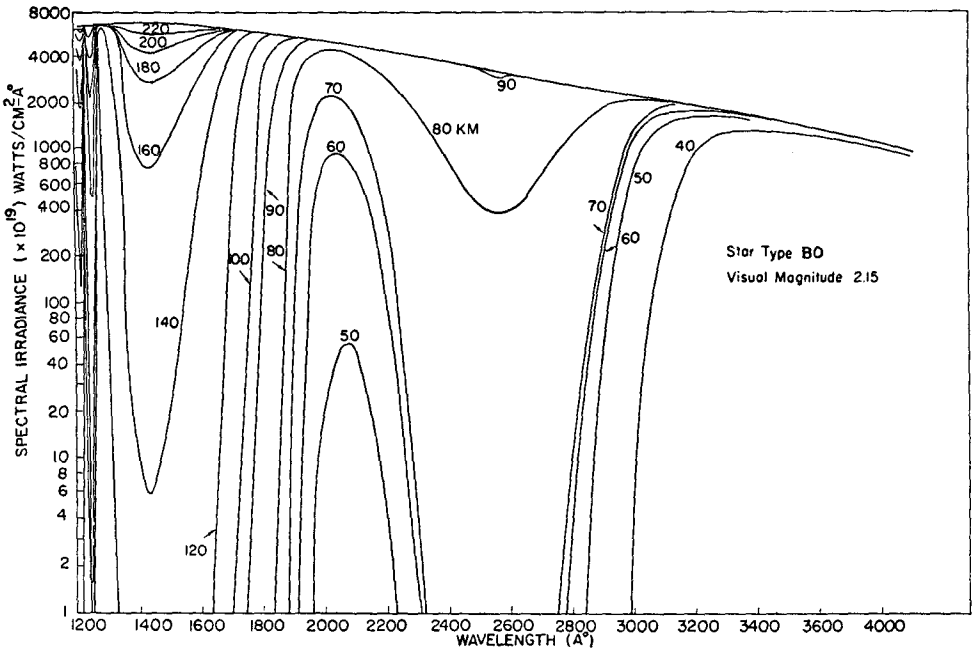

FIG. 15. Ultraviolet stellar spectra for various tangent ray heights during occultation with molecular scattering, molecular oxygen absorption, and ozone absorption (the Hunt nighttime profile of Fig. 12).

near the ultraviolet region of interest. To show typical transmission spectra, we have chosen the star γCas, a class BO star, with an effective blackbody temperature of 21,000K and a visual magnitude of 2.15 (Allen, 1963), and have calculated the transmission spectra at various altitudes during occultation. These transmission spectra are shown in Fig. 15 where the intital blackbody distribution is seen to be altered and attenuated as a result of molecular oxygen absorption in the region 100–250 km and by the combined effects of molecular oxygen absorption, Rayleigh scattering, and ozone absorption in the region 40–100 km. The Hunt nighttime ozone profile was used in these calculations.

7. Vertical profiles of absorbing species from spectral data

The stellar spectra calculated for the models discussed in the previous sections contain in their detail an enormous amount of information about the atmosphere. An interesting possibility exists for extracting this information from occultation data; that is, determining vertical profiles of the attenuating species directly from measurements of the transmitted spectra. Consider the transmission function for a particular absorbing species, i.e.,

$$T_i(r_0\lambda)=\exp\left\{-2\sigma_i(\lambda)\int_{r_0}^{\infty}\frac{N_i(r)rdr}{\sqrt{r^2-r_0^2}}\right\}, \qquad (22)$$

which can be written as the integral equation

$$\int_{r_0}^{\infty}\frac{N_i(r)rdr}{\sqrt{r^2-r_0^2}}=\log\left[\frac{1}{T_i(r_0,\lambda)}\right]^{2\sigma_i(\lambda)}. \qquad (23)$$

We note that Eq. (23) is an Abel integral equation of outwardly the same nature as the refraction equation (1) and, consequently, can be inverted to yield the number density $N_i(r)$ in the form

$$N_i(r)=\frac{1}{2\pi\sigma_i(\lambda)}\frac{d}{dr}\left\{\int_r^{\infty}\left(\frac{r}{r_0}\right)\frac{\log[T_i(r_0,\lambda)]dr_0}{\sqrt{r_0^2-r^2}}\right\}. \qquad (24)$$

The use of a point source, as a star, is important since in the absence of refraction at high altitudes all rays reaching the satellite must pass through the same tangent point, thus giving a very fine atmospheric probe.

Thus, if we were to measure the intensity of the stellar spectra even at relatively isolated wavelengths, for a series of tangent ray heights as a star is occulted, it would be possible to invert the data and retrieve vertical

profiles of the number density of the absorbing gases. The spectral resolution required depends upon the altitude range over which the profile would be measured and, of course, on the number of unknown absorbers that must be separated. The process of inversion would in general be iterative and subject to some error due to the lack of knowledge concerning the cross sections for the various absorption processes. As a practical note, it is interesting to point out that only the relative change of intensity of the starlight is required if there are no intense emission lines in the stellar spectral region of interest and that if a region where the cross section is relatively constant is used, even emission lines become unimportant.

Consider again the visible and ultraviolet spectral regions. In the lower atmosphere where ozone, scattering and refractive dispersion affect the visible spectrum, one can recover the ozone and Mie scatter density profiles after removing the effects of Rayleigh scattering and refractive dispersion which are relatively predictable. This has been attempted previously using sunlight reflected by an occulting satellite. Venkateswaran *et al.* (1961) sought to recover the ozone density profile near sunset in this manner; however, the sun subtends such a large angle at the earth that the broadening at the tangent point degrades the results. The technique used by Venkateswaran *et al.* was to obtain photometric data in two narrow spectral regions, one lying in the center of the Chappuis absorption band and the other nearby, but away from, the peak absorption. Thus, the effects of scattering and refractive dispersion are, in principle, monitored and removed by subtraction of the data in two spectral regions. This technique is useful and could be extended by using several isolated bands chosen to monitor the important scattering and attenuation effects, but starlight would be a preferable probe.

The stellar ultraviolet spectrum for light transmitted through the upper mesosphere and thermosphere is affected primarily by ozone and molecular oxygen. Not only are these effects predominately restricted to two spectral regions, but also, from the previous discussion, the altitudes for which there is uncertainty in the number density of each species are distinct. The obvious implication is that between 100 and approximately 250 km, the molecular oxygen density can be recovered using spectral data from a region centered at about 1450Å. Possibly a single broadband photometer would suffice since the cross section is relatively constant near 1450Å; thus, variations in the undistorted stellar spectrum would not be important. The Shumann-Runge band system should, of course, be avoided. At lower altitudes, from about 50–100 km, there are two spectral regions of interest in determining the high level ozone profile, one near 2100Å and a second near 2500Å. Again photometric measurements of relatively low resolution would cover the desired altitude range and be insensitive to the shape of the undistorted stellar spectrum. The effects of Rayleigh scattering and molecular oxygen would have to be removed at low altitudes, but this should not be serious since both the total number density and the molecular oxygen density are predictable below 100 km.

Acknowledgments. The work was supported by the National Aeronautics and Space Administration through Contract NASr-54(08), and the National Science Foundation through Grant GA-1025.

REFERENCES

Allen, C. W., 1963: *Astrophysical Quantities,* 2nd ed. The Athlone Press, University of London, 291 pp.

Bateman, H., 1910: The solution of the integral equation connecting the velocity of propagation of an earthquake wave in the interior of the earth with the times which the disturbance takes to travel to the different stations on the earth's surface. *Phil. Mag.*, **19**, 576–587.

Baum, W. A., and A. D. Code, 1953: A photometric observation of the occultation of Sigma Arietis by Jupiter. *Astron. J.*, **58**, 108–112.

Chagnon, C. W., and C. E. Junge, 1961: The vertical distribution of submicron particles in the stratosphere. *J. Meteor.*, **18**, 746–752.

Colegrove, F. D., F. S. Johnson and W. B. Hanson; 1966: Atmospheric composition in the lower thermosphere. *J. Geophys. Res.*, **71**, 2227–2235.

Ditchburn, R. W., and P. A. Young, 1962: The absorption of molecular oxygen between 1850 and 2500 Å. *J. Atmos. Terr. Phys.*, **24**, 127.

Fischbach, F. F., 1965: A satellite method for pressure and temperature below 24 km. *Bull. Amer. Meteor. Soc.*, **46**, 528–532.

Green, A. E. S., 1964: Attenuation by ozone and the earth's albedo in the middle ultra-violet, *Appl. Opt.*, **3**, 203–208.

Hays, P. B., and R. G. Roble, 1968: Atmospheric properties from the inversion of planetary occultation data. *Planetary Space Sci.*, **16**, 1197.

Hinteregger, H. E., and L. A. Hall, 1965: Solar XUV radiation and neutral particle distribution in July 1963 thermosphere. *Space Research V*, Amsterdam, North-Holland Publishing Co., 1248 pp.

Hunt, B. G., 1966: Photochemistry of ozone in a moist atmosphere. *J. Geophys. Res.*, **71**, 1385–1397.

Johnson, F. S., J. D. Purcell and R. Tousey, 1951: Measurements of the vertical distribution of atmospheric ozone from rockets. *J. Geophys. Res.*, **56**, 583–594.

Jones, L. M., F. F. Fischbach and J. W. Peterson, 1962: Satellite measurements of atmospheric structure by refraction. *Planetary Space Sci.*, **9**, 351–352.

Junge, C. E., 1963: Air Chemistry and Radioactivity. *Interna-*

tional Geophysics Series, Vol. 4, New York, Academic Press, 118–142.

London, J., 1967: The average distribution and time variation of ozone in the stratosphere and mesosphere. *Space Research VII*, Amsterdam, North-Holland Publishing Co., 172–183.

Pannekoek, A., 1903: Uber die Eracheinungen, welche bei einer Sternbedeckung durch einen Planeten auftreten. *Astron. Nach.*, **164**, 5–10.

Roney, P. L., 1965: On the influence of water vapor on the distribution of stratospheric ozone. *J. Atmos. Terr. Phys.*, **27**, 1177–1190.

van de Hulst, H. C. 1962: *Light Scattering by Small Particles*, 2nd ed. New York, John Wiley, 176 pp.

Venkateswaran, S. V., J. G. Moore and A. J. Krueger, 1961: Determination of the vertical distribution of ozone by satellite photometry. *J. Geophys. Res.*, **66**, 1751–1771.

Watanabe, K., 1958: Ultra-violet absorption process in the upper atmosphere. *Advances in Geophysics*, Vol. 5, New York, Academic Press, 325 pp.

Weisberg, H. L., 1962: The study of planetary atmospheres by stellar occultation. Jet Propulsion Laboratory, Memo. RM-32790JPL, 40 pp.